Molecular Biology of the Cell
Vol. 15, 3542–3552, August 2004

Characterization of a Nonclathrin Endocytic Pathway: Membrane Cargo and Lipid Requirements[D]

Naava Naslavsky,* Roberto Weigert,* and Julie G. Donaldson†

Laboratory of Cell Biology, National Heart, Lung, and Blood Institute, National Institutes of Health, Bethesda, Maryland 20892

Submitted February 24, 2004; Revised April 22, 2004; Accepted May 5, 2004
Monitoring Editor: Howard Riezman

Clathrin-independent endocytosis internalizes plasma membrane proteins that lack cytoplasmic sequences recognized by clathrin adaptor proteins. There is evidence for different clathrin-independent pathways but whether they share common features has not been systematically tested. Here, we examined whether CD59, an endogenous glycosylphosphatidyl inositol-anchored protein (GPI-AP), and major histocompatibility protein class I (MHCI), an endogenous, integral membrane protein, entered cells through a common mechanism and followed a similar itinerary. At early times of internalization, CD59 and MHCI were found in the same Arf6-associated endosomes before joining clathrin cargo proteins such as transferrin in common sorting endosomes. CD59 and MHCI, but not transferrin, also were observed in the Arf6-associated tubular recycling membranes. Endocytosis of CD59 and MHCI required free membrane cholesterol because it was inhibited by filipin binding to the cell surface. Expression of active Arf6 stimulated endocytosis of GPI-APs and MHCI to the same extent and led to their accumulation in Arf6 endosomes that labeled intensely with filipin. This blocked delivery of GPI-APs and MHCI to early sorting endosomes and to lysosomes for degradation. Endocytosis of transferrin was not affected by any of these treatments. These observations suggest common mechanisms for endocytosis without clathrin.

INTRODUCTION

Cells sample their environment and internalize plasma membrane through the general process of endocytosis. Endocytosis can be divided into clathrin-dependent and clathrin-independent processes. Clathrin-dependent endocytosis is well characterized and involves the selective uptake of plasma membrane proteins containing cytoplasmic sorting sequences via the recruitment of AP2 or other adaptor proteins, clathrin, and a host of accessory proteins that facilitate vesicle budding and fission (Slepnev and De Camilli, 2000; Conner and Schmid, 2003).

Clathrin-independent mechanisms encompass pinocytosis, macropinocytosis, and phagocytosis (Johannes and Lamaze, 2002; Conner and Schmid, 2003) with macropinocytosis and phagocytosis representing stimulated processes driven by the cortical actin cytoskeleton. These processes have not been thoroughly characterized nor have their relationships with each other been clarified. The discovery that certain membrane proteins can reside in cholesterol and sphinogolipid-rich microdomains that are resistant to detergent extraction led to enormous interest in studying the trafficking of these proteins and their mechanism of internalization (Ikonen, 2001). In particular, the trafficking of proteins anchored to the membrane by a glycosylphosphatidyl inositol (GPI) moiety has been the focus of many studies. There is general agreement that the internalization of GPI-anchored proteins (GPI-APs) is both clathrin and, usually, dynamin independent (Skretting *et al*., 1999; Ricci *et al*., 2000; Nichols *et al*., 2001; Sabharanjak *et al*., 2002) and thought to not involve caveolae (Sabharanjak *et al*., 2002; Nabi and Le, 2003; Parton and Richards, 2003). Once internalized, GPI-APs have been observed to recycle back to the plasma membrane (PM) via the juxtanuclear endocytic recycling compartment (Fivaz *et al*., 2002; Sabharanjak *et al*., 2002) or to be transported from early to late endosomes (Fivaz *et al*., 2002). In some cases, a trafficking route from the PM to the Golgi has been observed in COS cells (Nichols *et al*., 2001). In contrast to GPI-AP, trafficking back to the Golgi has consistently been observed for other raft-associated proteins, notably, ganglioside-bound toxins such as Cholera and Shiga (Torgersen *et al*., 2001).

We have characterized a clathrin-independent endocytic pathway that traffics integral membrane proteins lacking cytoplasmic AP2/clathrin-sorting sequences. The Arf6 GTPase is associated with these membranes and modulates their trafficking through the pathway (Radhakrishna and Donaldson, 1997; Brown *et al*., 2001; Naslavsky *et al*., 2003). Among the proteins entering cells through this pathway are the major histocompatibility complex class I protein (MHCI), the interleukin-2 (IL2) receptor α subunit (Tac) (Radhakrishna and Donaldson, 1997; Naslavsky *et al*., 2003), integrins (Brown *et al*., 2001; Powelka *et al*., 2004), and E-cadherin (Paterson *et al*., 2003). After entry in distinct vesicles that do not contain clathrin-derived cargo, MHCI-containing vesicles soon fuse with EEA1-positive endosomes that contain clathrin cargo such as low-density lipoprotein and transferrin. Some MHCI recycles along Arf6-associated tubular endosomes back to the PM (Caplan *et al*., 2002; Powelka *et al*., 2004), whereas some proceeds on to late endosomes/lysosomes for degradation (Naslavsky *et al*., 2003).

Article published online ahead of print. Mol. Biol. Cell 10.1091/mbc.E04–02–0151. Article and publication date are available at www.molbiolcell.org/cgi/doi/10.1091/mbc.E04–02–0151.

[D] Online version of this article contains supporting material. Online version is available at www.molbiolcell.org.

* These authors contributed equally to this work.
† Corresponding author. E-mail address: jdonalds@helix.nih.gov.

Having described the clathrin-independent endosomal system that is associated with Arf6, we wished to expand our knowledge of this endocytic pathway. In particular, whether detergent-resistant membrane proteins, such as GPI-anchored proteins, would traffic in this pathway and whether we could define the requirements for endocytosis without clathrin.

MATERIALS AND METHODS

Cells and Cell Culture

HeLa cells were grown in DMEM supplemented with 10% fetal bovine serum, 100 μg/ml streptomycin, and 100 U/ml penicillin.

Plasmids and Transient Transfection

Tac-GPI was a kind gift from J. Bonifacino (National Institutes of Health, Bethesda, MD). Tac-GPI is a chimeric protein constructed by fusing the extracellular domain of the human Tac antigen (α chain of interleukin-2 receptor) with the signal peptide (nucleotides 617–735) of CD16, a GPI-anchored form of the Fcγ receptor (Delahunty *et al*., 1993). Tac-DKQTLL (Tac-LL) is a chimera of Tac, containing the cytoplasmic tail of the mouse CD3 described previously (Naslavsky *et al*., 2003). Arf6 and mutants are in pXS plasmid (Radhakrishna and Donaldson, 1997). DynII-K44A-GFP was from M. McNiven (Mayo Clinic, Rochester, MN). GFP-Rab5 and mutants are from R. Lodge (Laval, Quebec, Canada). For transfection, cells were plated and transfected the next day using FuGENE (Roche Diagnostics, Indianapolis, IN). Experiments were performed 17–20 h after transfection.

Reagents and Antibodies

Rabbit polyclonal antibody to Arf6 was described previously (Song *et al*., 1998) and anti-caveolin-1 was from BD Transduction Laboratories (Lexington KY). Mouse monoclonal antibody to human MHCI (W6/32) and Tac (7G7) were described previously (Naslavsky *et al*., 2003). Cy3- and Cy5-conjugated anti-MHCI (W6/32) antibodies were prepared with FluorolinkM antibody Cy3- and Cy5-labeling kit (Amersham Biosciences, Piscataway, NJ). Rabbit-anti-Tac (from W. Leonard, National Institutes of Health) was used in Western blot to detect biotinylated Tac. Unconjugated and fluorescein isothiocyanate (FITC)-conjugated anti-CD59 antibodies were purchased from Chemicon (Melbourne, Australia) and R-phycoerythrin–conjugated anti-CD59 was from Leinco (St. Louis, MO). Biotinylated anti-Tac (CD25, clone 143-13) was purchased from BioSource International (Camarillo, CA). Molecular Probes (Eugene, OR) was the source for dextran (10,000) conjugated to Alex 594; transferrin (Tfn) conjugated to Alexa 488, 594, and 633; and all secondary antibodies conjugated to 594, 488, and 647. Filipin and dextran were from Sigma-Aldrich (St. Louis, MO) and Biotin-X-NHS was from Calbiochem (San Diego, CA). Streptavidin beads, donkey anti rabbit-horseradish peroxidase, and chemiluminescence kit were from Pierce Chemical (Rockford, IL).

Immunofluorescence and Confocal Analysis

Cells were plated on glass coverslips and transfected the next day. For uptake of Tfn, untransfected cells were serum starved for 30 min at 37°C in DMEM containing 0.5% bovine serum albumin (BSA), and then fluorescently labeled Tfn was added. For triple cargo internalization assays (Figure 1), Cy3-anti-MHCI (30–50 μg/ml) and FITC-conjugated anti-CD59 (1:10) also were used. Uptake of anti-Tac antibody was performed in complete media at 37°C for the indicated time. In all internalization experiments, at the end of incubation, PM-associated ligand and antibodies were removed by rinsing the cells in low pH solution (0.5% acetic acid, 0.5 M NaCl, pH 3.0) for 45 s. PM-associated anti-CD59 (FITC) was stripped for 90 s with 100 mM glycine, 20 mM magnesium acetate, 50 mM KCl, pH 2.2. Cells were then fixed with 2% formaldehyde/phosphate-buffered saline (PBS) at room temperature (RT) for 10 min and stained in blocking solution (PBS containing 10% fetal calf serum and 0.2% saponin). The internalized antibodies were visualized with the appropriate secondary antibodies. In experiments for uptake in the presence of filipin, untransfected cells were pretreated with DMEM supplemented with 0.5% BSA, with or without 12 μg/ml filipin for 30 min before the antibody addition. All images were obtained using a 510 LSM confocal microscope (Carl Zeiss, Thornwood, NY) with 63× Plan Apo objective as described previously (Naslavsky *et al*., 2003). Acquisition of figures was accomplished in Adobe Photoshop 5.5.

Quantification of Total Immunofluorescence

Thirty to 50 cells per coverslip were randomly selected and imaged using a 510 LSM confocal microscope (Carl Zeiss) with a 40× plan Apo objective. The pinhole was completely open, and all the images were taken with identical acquisition parameters, those previously optimized for the fluorescent signals to be in the dynamic range. Under these conditions the amount of cargo internalized per cell is proportional to the total fluorescence. For each channel, the total fluorescence of each individual cell was measured using the LSM image examiner (version 3.01; Carl Zeiss).

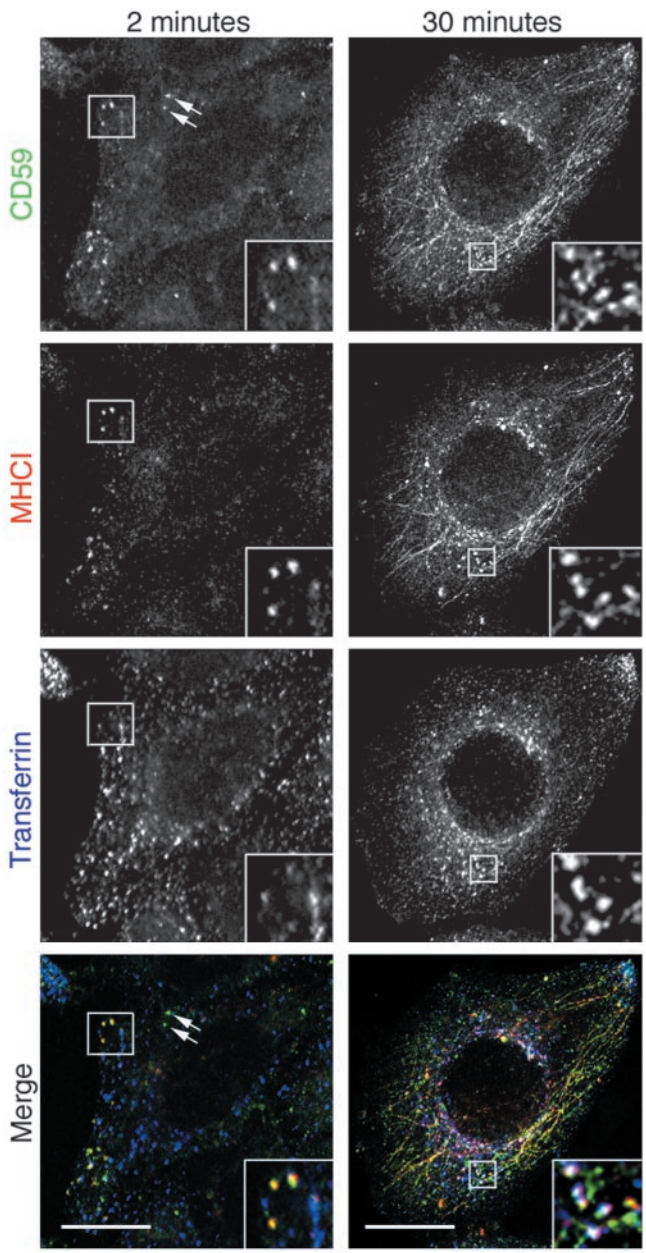

Figure 1. Internalization of CD59, MHCI, and transferrin in untransfected cells. HeLa cells were incubated at 37°C as described in MATERIALS AND METHODS with FITC-anti-CD59 (green), Cy3-anti MHCI (red), and 5 μg/ml Alexa 633-transferrin (blue) for 2 min and 30 min. PM-associated ligands were removed by low pH treatment before fixation. Inset shows endosomes containing CD59 and MHCI (yellow) at 2 min and endosomes containing CD59, MHCI and transferrin (white) at 30 min. Some endosomes at 2 min only contain CD59 (arrows). Bar, 10 μm.

Internalization Assay: Cell Enzyme-linked Immunosorbent Assay (CELISA)

A cell-based enzyme-linked immunosorbent assay was used to measure the internalized biotinylated Tac antibody. HeLa cells were plated in a 24-well dishes at a concentration of 100,000 cells/well and transfected the next day with different plasmids (0.2 μg/well) by using 0.9 μl/well FuGENE. Each time point was performed in triplicate. Cells transfected with either Tac-GPI,

Tac, or Tac-LL, with or without coexpression of the active mutant of Arf6, were incubated at 37°C for different times with biotinylated anti-Tac antibody. At each time point, the internal pool of Tac antibody was assessed by removing the biotinylated anti-Tac from the PM with a 45-s rinse in low pH solution (0.5% acetic acid, 0.5 M NaCl pH 3.0), followed by thorough washes with PBS. Samples were fixed with 2% formaldehyde/PBS for 10 min at RT. A parallel triplicate at each time point was immediately fixed, to provide the total amount of cell-associated Tac antibody. The internal pool (acid stripped) was calculated as a percentage of the total cell-associated (nonstripped) at each time point. In Figure 4A, cells were preincubated at 37°C in DMEM/0.5% BSA, with or without 12 μg/ml filipin for 20 min before the addition of the biotinylated anti-Tac antibody (diluted in DMEM/0.5% BSA). Biotinylated antibodies were detected with 0.1 μg/ml streptavidin-HRP prepared in 5% BSA/PBS containing 0.2% saponin for 45 min at room temperature. Colorimetric reaction (O.D. 450) was carried out with tetramethylbenzidine peroxidase substrate and stop solution from BioFX Laboratories (Rotterdam, Holland).

Degradation Assay

Biotinylation and immunoprecipitation were performed as described previously (Naslavsky *et al*., 2003) with some modifications. Briefly, HeLa cells transfected with Tac-GPI were washed with cold PBS and labeled with 0.3 mg/ml Biotinoyl amidocapronic acid *N*-hydroxysuccinimide ester for 30 min on ice, and then incubated for the indicated time with complete media at 37°C and lysed in lysis buffer (25 mM Tris, pH 7.5, 150 mM NaCl, 5 mM EDTA, 0.5% Triton X-100 [TX-100], 0.25% sodium deoxycholate). Biotinylated proteins were immunoprecipitated with streptavidin beads, separated on SDS-PAGE, and biotinylated Tac-GPI was detected in Western blot by using rabbit anti-Tac, followed by donkey anti-rabbit conjugated to HRP. For detection, we used chemiluminescence (Pierce Chemical, Rockford, IL).

Visualizing Cholesterol with Filipin

Cells were stained with filipin as described previously (Holtta-Vuori *et al*., 2002). The cells were fixed for 20 min with 4% formaldehyde and quenched with 50 mM NH_4Cl for 10 min, and then incubated at RT with PBS supplemented with 10% fetal bovine serum, 0.2% saponin, and 2 mM final concentration of filipin. A 50 mg/ml stock of filipin was prepared in dimethyl sulfoxide and stored in small aliquots because filipin looses its fluorescence upon repeated thawing. Unbound filipin was removed by extensive washes with PBS. Images of filipin were immediately captured on a charge-coupled device camera attached to an epifluorescence photomicroscope (Carl Zeiss) with a 63×/1.4 Plan Apo chromate objective, which has transmittance in the UV region. A UV filter cube (365-nm excitation, 405-nm emission) permitted visualization of filipin, whereas standard rhodamine and fluorescein filters cubes were used as red and green channels accordingly, to image the costained fluorophores. No autofluorescence was detected with the UV filter because cells that were not stained with filipin had no signal.

Triton X-100 Extraction of Live Cells

HeLa cells plated on glass coverslips, cotransfected with Arf6-Q67L and Tac-GPI, were allowed to internalize anti-Tac antibody for 1 h at 37°C in complete media. They were then were stripped, cooled, and treated with 1% TX-100 (vol/vol in PBS) on ice for 3 min, and fixed as described above.

RESULTS

CD59 and MHCI Share the Same Endocytic Pathway

To follow the entry of three types of plasma membrane proteins, we simultaneously examined the internalization of CD59 (a GPI-AP), MHCI, and the transferrin receptor. We confirmed that CD59 can be classified as a "raft", detergent-resistant protein because it was resistant to extraction by cold TX-100. By contrast, MHCI was fully solubilized by this treatment (see Supplementary Figure 1) as is the transferrin receptor (Hao *et al*., 2004), thus indicating that these integral membrane proteins, MHCI, and the transferrin receptor do not share this characteristic. All three are endogenous proteins in HeLa cells. The endocytosis of CD59 and MHCI was monitored by following internalization of bound fluorophore-conjugated antibodies and that of transferrin receptor by fluorophore-conjugated transferrin. After 2 min of internalization, some CD59-labeled endocytic structures colabeled with antibody to MHCI (Figure 1, 2 min; see inset) and some structures contained CD59 alone (Figure 1, 2 min; arrows), but few, if any, colabeled with transferrin. At 30 min, endosomes containing CD59, MHCI, and transferrin were observed, especially in the juxtanuclear region (Figure 1, 30 min; inset). At 30 min of internalization, CD59 and MHCI, but not transferrin, were observed colocalized in tubular membranous structures that emanated from the juxtanuclear region (Figure 1, 30 min). These tubular endocytic structures are observed in ~40–60% of HeLa cells (our unpublished observations), they have Arf6 associated with them, are devoid of transferrin, and as such, are hallmarks of this clathrin-independent endosomal membrane system (Radhakrishna and Donaldson, 1997). Similar patterns of internalization were observed for other GPI-APs such as Tac-GPI, a chimeric protein consisting of the extracellular portion of Tac (the IL2 receptor α subunit) that is anchored to the membrane through a GPI appendage (our unpublished observations; see below) and for the folate receptor (our unpublished observations). These observations suggest that CD59 and MHCI occur in the same early endocytic structure before fusion with transferrin-containing early endosomes and that, at later times, CD59 and MHCI also can be observed in the same, tubular endosome that represents the route of recycling back to the PM (Radhakrishna and Donaldson, 1997; Caplan *et al*., 2002).

The colocalization of CD59 and MHCI in the same early endosome suggested that the two PM proteins might be internalized by a common mechanism. Neither CD59 nor MHCI is expected to be affected by expression of mutant constructs that affect clathrin function. To confirm this, we expressed the carboxyl-terminal domain of AP180 (C-AP180), a truncated protein that inhibits clathrin endocytosis by sequestering clathrin (Zhao *et al*., 2001), and examined its effect on internalization of CD59, MHCI and transferrin. As shown in Figure 2, the amount of CD59 and MHCI internalized was not affected by expression of C-AP180 (Figure 2A), whereas transferrin endocytosis was severely impaired (Figure 2B). Interestingly, we observed that the distribution of MHCI and CD59 endosomes was more concentrated in the juxtanuclear region in cells expressing C-AP180 than in untransfected cells. We quantified the effect of expression of C-AP180 on internalization of the three cargo proteins and found that transferrin internalization was reduced by half, whereas CD59 and MHCI uptake was similar in transfected and untransfected cells (Figure 2E). In addition to clathrin-independence, the internalization of CD59 and other GPI-APs into HeLa and COS cells is independent of dynamin function (Nichols *et al*., 2001; Sabharanjak *et al*., 2002) (our unpublished observations) as is the internalization of MHCI (Naslavsky *et al*., 2003).

Because CD59 and other GPI-APs are proteins that can reside in detergent-resistant membrane domains, we expected that the internalization of CD59 would be sensitive to cholesterol-sequestering protocols and wondered whether the internalization of MHCI also would be affected by these treatments. The extraction of cholesterol by the use of β-cyclodextrin (Brown, 2002) is one means to perturb PM cholesterol, but this approach also can lead to disruption of clathrin-dependent pathways (Rodal *et al*., 1999) and alteration in the lateral mobility of PM proteins (Kwik *et al*., 2003). Instead, the ability of filipin to bind to and sequester PM cholesterol in the membrane of living cells was used to assess whether pretreatment with this reagent had an effect on endocytosis (Awasthi-Kalia *et al*., 2001). The endocytosis of both CD59 and MHCI was significantly inhibited in the presence of filipin (Figure 2, C and D), although filipin did not prevent antibody binding to the cell surface at 4°C (our unpublished observations). By contrast, the amount of transferrin internalized was not affected by filipin (Figure 2, C and D), although the distribution of transferrin-containing

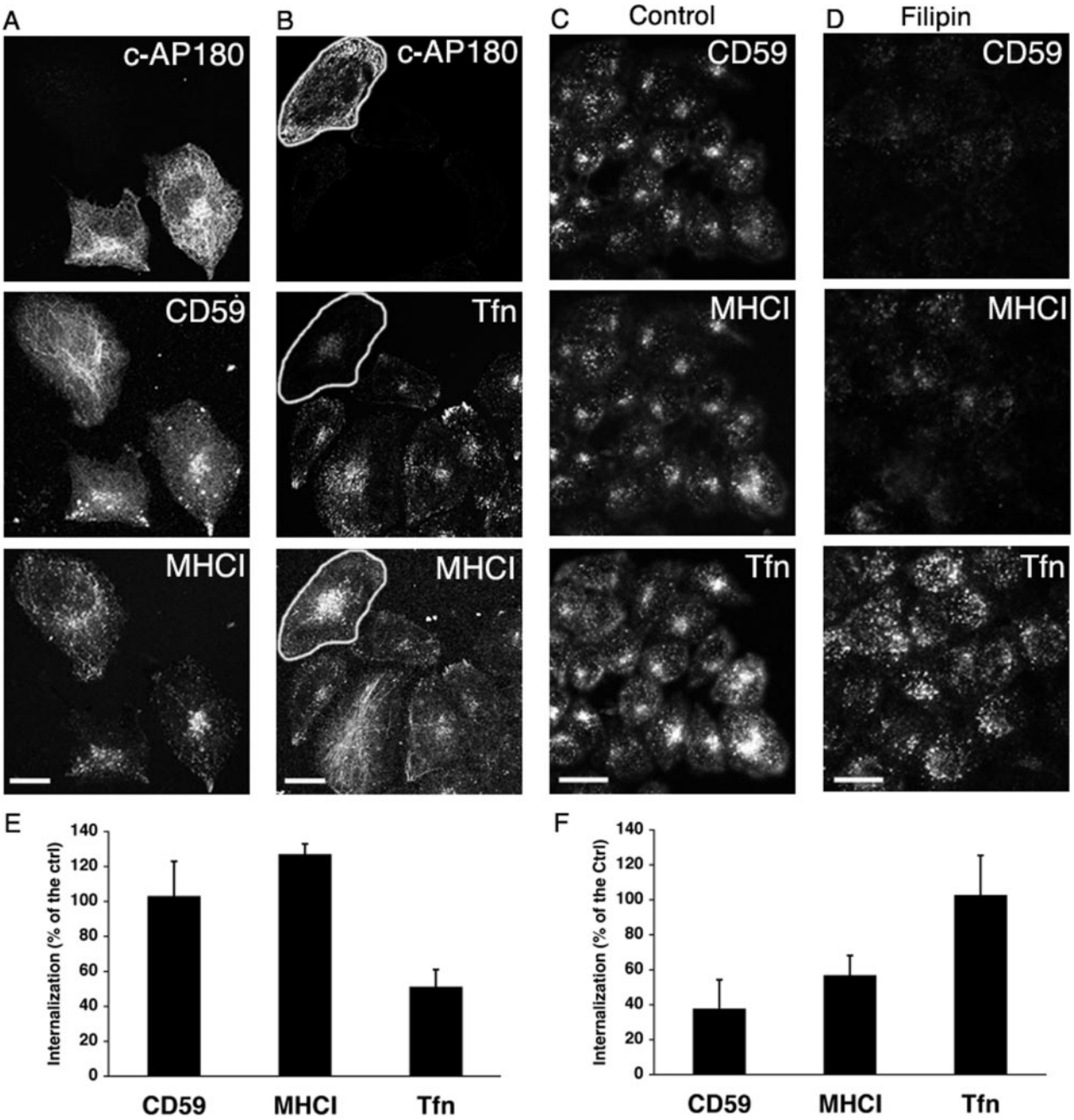

Figure 2. Effect of endocytosis inhibitors on CD59 and MHCI internalization. (A and B) HeLa cells were transfected with FLAG-c-AP180 and internalization of anti-CD59 and anti-MHCI (A) or of anti-MHCI and Tfn (B) was assessed. (C and D) Untransfected HeLa cells were preincubated for 20 min at 37°C with DMEM containing 0.5% BSA in the absence (C) or presence (D) of filipin (12 μg/ml). Then, Cy5-anti MHCI, R-phycoerythrin-anti-CD59, and Alexa 488-Tfn (5 μg/ml) were added for a 20-min uptake. The cells were fixed and processed for immunofluorescence. All images were taken with identical acquisition parameters and the amount of internalized antibody for either c-AP180 (E) or filipin treatment (F) was measured and expressed as a percentage of that internalized in control cells (see MATERIALS AND METHODS). Bar, 10 μm (A and B) and 20 μm (C and D).

endosomes was more dispersed in filipin-treated cells. Filipin treatment inhibited CD59 and MHCI endocytosis by ~60 and 50%, respectively (Figure 2F). These experiments demonstrated that CD59 and MHCI endocytosis required free PM cholesterol and was not affected by inhibitors of clathrin or dynamin function.

Previously, we demonstrated that MHCI is an endogenous membrane protein that enters cells independently of dynamin and clathrin and travels in endosomes that can be labeled with antibody to Arf6 in cells overexpressing Arf6 (Naslavsky *et al.*, 2003). Because Arf6 expression is very low in HeLa cells (Song *et al.*, 1998), localization of the endogenous protein is difficult to achieve with existing immunological reagents. We have found that the overexpression of wild-type Arf6 has no observable effect on the trafficking or morphology of endosomal systems in HeLa cells

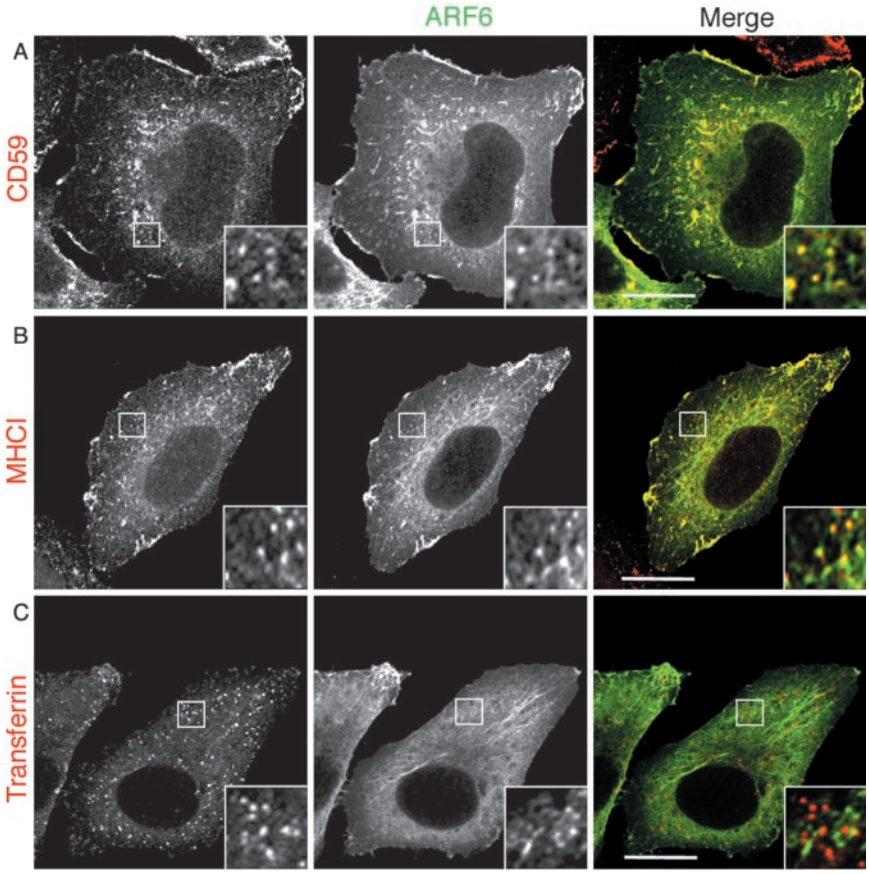

Figure 3. CD59 and MHCI colocalize with Arf6 at early times of internalization. HeLa cells were transfected with Arf6 (wild type) and allowed to internalize for 2 min either unlabeled anti-CD59 (A) or unlabeled anti-MHCI (B), or Alexa-594-Tfn (C). (A and B) Cells were fixed and incubated for 1 h with goat anti-mouse total IgG in the absence of saponin to mask the surface bound antibodies. Cells were fixed again for 5 min, blocked, and incubated with the rabbit polyclonal antibody against Arf6 in the presence of saponin. Alexa 488-goat anti rabbit IgG and Alexa 594 goat anti-mouse IgG were used as secondary antibodies to reveal Arf6 and MHC or CD59 respectively. Cells were probed for Arf6 as described in MATERIALS AND METHODS. Bar, 10 μm.

(Radhakrishna and Donaldson, 1997; Brown *et al*., 2001; Naslavsky *et al*., 2003), and so we have used moderate levels of expression to localize Arf6-containing membranes. Observing CD59 and MHCI in common structures devoid of transferrin at 2 min of internalization led us to examine whether CD59 enters cells in Arf6-associated endosomes. After 2-min internalization, many CD59-labeled punctate structures also labeled with antibody to Arf6 (Figure 3A, inset); MHCI labeled endosomes also colocalized with Arf6 (Figure 3B, inset). By contrast, after 2 min of internalization, transferrin-containing endosomes did not label with antibody to Arf6 (Figure 3C, inset).

Endocytosis of GPI-APs and Clathrin-independent Integral Membrane Proteins Is Stimulated by Activated Arf6

Because CD59 and MHCI were internalized in the same Arf6-associated vesicle, we wished to determine whether their internalization would be affected to the same extent by expression of constitutively active or inactive mutants of Arf6. We developed a quantitative assay to monitor internalization from the PM of Tac chimeras that represent the three types of cargo proteins: Tac for MHCI, Tac-GPI for CD59, and Tac-LL, with a dileucine motif that renders the protein competent for clathrin-mediated endocytosis similar to transferrin (Naslavsky *et al*., 2003). To perform these experiments, we monitored the internalization of a biotinylated Tac antibody into the cells by using a CELISA (see MATERIALS AND METHODS). Because all three cargo proteins were monitored using the same Tac antibody and because the frequency of coexpression of the Tac chimeras with the Arf6 proteins is high, the rates of antibody internalization could be directly compared and would reflect the rates of internalization for the different Tac chimeras.

We first examined the effect of different Arf6 constructs on the internalization of Tac antibody into cells expressing Tac-GPI, Tac, or Tac-LL. Looking at 20-min internalization, a time early enough that little recycling should be occurring (Caplan *et al*., 2002), overexpression of wild-type Arf6 had no significant effect on the uptake of any of the Tac proteins (Figure 4A, compare white to black bars). Remarkably, expression of Arf6-Q67L increased internalization of both Tac-GPI and Tac approximately twofold while having no effect on internalization of Tac-LL (Figure 4A, red bars). The stimulation of internalization in cells expressing Arf6-Q67L was not restricted to Tac-containing constructs, because endocytosis of MHCI was stimulated to the same extent (our unpublished observations). It is important to note that the stimulated internalization of Tac and Tac-GPI caused by Arf6-Q67L occurs at early times (16–20 h) of transfection. At these early times of expression of activated Arf6, clathrin-independent cargo enters cells and accumulates in intracellular vesicles, whereas at later times (greater than 24 h) of expression, as vacuoles accumulate in the cells, endocytosis of MHCI is halted (Radhakrishna and Donaldson, 1997; Brown *et al*., 2001).

We examined this stimulatory effect of Arf6-Q67L in more detail during a time course of internalization. In cells expressing either Tac-GPI (Figure 4B, black circles) or Tac (Figure 4B, black triangles) alone, Tac antibody entered cells at a steady rate (1%/min). A striking acceleration of Tac-GPI and Tac endocytosis (to 4%/min) was observed in cells

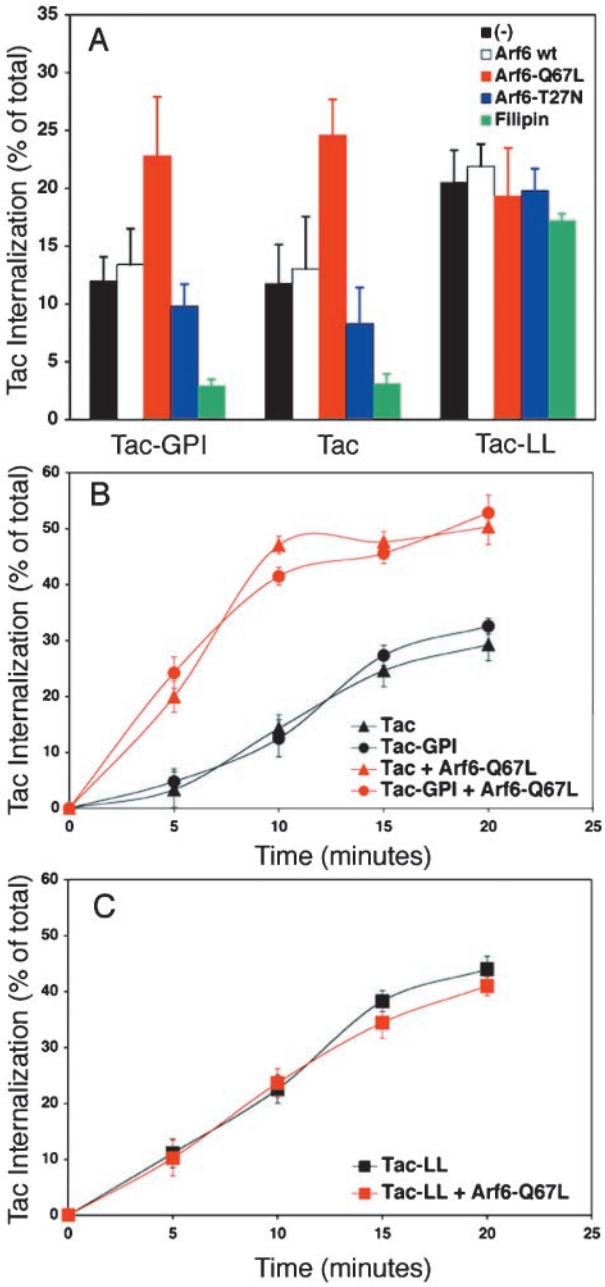

Figure 4. Accelerated endocytosis of GPI-AP and clathrin-independent cargo into Arf6-Q67L expressing cells. (A) Cells transfected with Tac-GPI, Tac or Tac-LL alone (black bars) or in combination with Arf6-wt (white bars), Arf6-Q67L (red bars), or Arf6-T27N (blue bars) were incubated with biotinylated anti-Tac for 20 min at 37°C. Cells expressing Tac-GPI, Tac, or Tac-LL also were treated with filipin before Tac-antibody internalization (green bars). The surface-bound antibody was then removed by a low pH solution rinse, and the sample was fixed and processed for CELISA (see MATERIALS AND METHODS). (B and C) Internalization of Tac-GPI and Tac (circles and triangles in B), and Tac-LL (squares in C) was measured in a continuous uptake by using CELISA. Cells expressing the cargo proteins alone (black symbols) or with Arf6-Q67L (red symbols) were incubated at 37°C with biotinylated anti-Tac for the indicated time and then processed as described above. The amount of internalized Tac antibody is expressed as a percentage of total cell-associated anti-Tac. This experiment was performed three times with similar results. Data are means of triplicates with SD.

coexpressing Arf6-Q67L (Figure 4B, red circles and red triangles, respectively). By contrast, the internalization of Tac-LL was linear for up to 20 min and the rate of internalization was not altered in cells expressing Arf6-Q67L (Figure 4C, black and red squares). Thus, by using the same antibody to measure internalization of Tac chimeras, both Tac-GPI and Tac entered cells at the same rate and were stimulated to the same extent by activated Arf6.

In contrast to the stimulated endocytosis observed with activated Arf6, expression of Arf6-T27N slightly decreased uptake of Tac-GPI and Tac (Figure 4A, blue bars) while barely influencing Tac-LL uptake (Figure 4A). This mild inhibition with Arf6-T27N suggests that Arf6 activity is not required for endocytosis. Filipin treatment, however, dramatically reduced internalization of Tac-GPI and Tac (Figure 4A, green bars) as well as MHCI (our unpublished observations) to 20% of untreated cells, whereas only a small decrease in Tac-LL internalization was observed with filipin treatment (Figure 4A, green bars). The response to filipin treatment observed in this biochemical assay is in agreement with the quantification of fluorescent antibody uptake for the endogenous proteins CD59 and MHCI shown in Figure 2F.

The observation that endocytosis of both Tac and Tac-GPI was affected by the same mutant of Arf6 supports the notion that these PM proteins, although capable of partitioning into different microdomains on the PM, enter the cell through common mechanisms.

CD59 and MHCI Become Trapped in Arf6 Early Endosomes in Cells Expressing Constitutively Active Arf6

We have previously shown that both MHCI and Tac accumulate in vacuolar structures in cells expressing Arf6-Q67L (Brown *et al*., 2001; Naslavsky *et al*., 2003). Because CD59 is internalized with MHCI and at accelerated rates in cells expressing Arf6-Q67L, we examined whether endogenous CD59 also would accumulate in these vacuolar structures. After 1 h of internalization, CD59 colocalized with Arf6-Q67L in these internal structures (Figure 5A). As mentioned above, endocytosed clathrin-independent cargo proteins could be trapped in these vacuoles during early (16- to 20-h) times of expression of Q67L, but not at later (>24 h) times (our unpublished observations) when extensive vacuolar accumulation leads to a block in internalization, as reported previously (Brown *et al*., 2001). We also could see the steady-state accumulation of both CD59 and MHCI within these vacuolar structures by total internal antibody labeling (Figure 5B). The steady-state accumulation of CD59 and MHCI in the vacuoles could be observed even at later times of transfection (our unpublished observations) when further endocytosis was halted. In addition to sequestering nonclathrin cargo, the Arf6Q67L vacuoles also contained fluid phase markers (Figure 5C), indicating that subsequent trafficking of both membrane and fluid was blocked in these cells. As previously shown (Brown *et al*., 2001; Naslavsky *et al*., 2003), neither low-density lipoprotein nor transferrin accumulated in these structures (our unpublished observations). Furthermore, in cells expressing both Dyn2K44A that blocked transferrin endocytosis and Arf6-Q67L that stimulated the internalization of nonclathrin cargo, transferrin still did not enter through this clathrin-independent pathway (Figure 5D). The accumulation of CD59 in vacuoles also was observed in COS and MCF-7 cells (our unpublished observations).

These observations show that both CD59 and MHC become trapped in Arf6-Q67L–associated vacuoles. We previously showed that Tac, like MHCI, is sequestered in such vacuolar structures and that Tac degradation is inhibited in

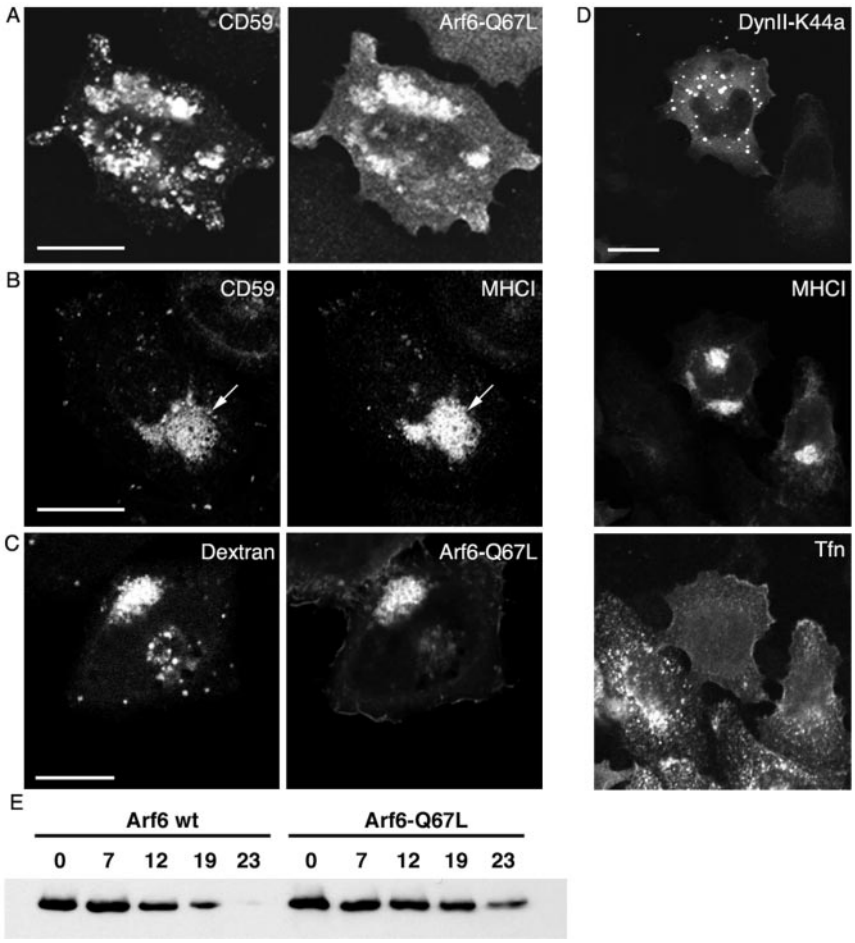

Figure 5. GPI-APs and fluid markers accumulate in vacuoles and degradation is inhibited in cells expressing Arf6-Q67L. (A) HeLa cells were transfected with Arf6-Q67L and were allowed to internalize anti-CD59 antibody at 37°C for 1 h, and then they were stripped, fixed, and processed for immunofluorescence. (B) HeLa cells expressing Arf6-Q67L were fixed, blocked, and the surface MHCI and CD59 masked by incubation for 1 h with unlabeled antibodies directed against MHCI and CD59 in the absence of saponin. Cells were then fixed again, blocked, and incubated for 1 h with FITC-conjugated anti-CD59 and Cy3-conjugated MHCI in the presence of saponin to stain for the internal pool of the two molecules. (C) HeLa cells were incubated with 20 mg/ml unlabeled dextran plus 0.5 mg/ml Alexa594-dextran during transfection with Arf6-Q67L for 16h. (D) Transferrin internalization (30 min) was assessed in HeLa cells that were cotransfected with DynII-K44A-GFP and Arf6-Q67L. After fixation cells expressing Arf6-Q67L were visualized with anti-MHCI staining of the vacuoles. Note that even in a cell expressing low levels of DynII-K44A (right-most cell), transferrin still will not enter into vacuolar membranes containing MHCI. (E) Half-life of surface Tac-GPI is lengthened in cells expressing Arf6-Q67L. HeLa cells were transfected with Tac-GPI and with either wild-type Arf6 or Arf6-Q67L. PM proteins were biotinylated for 30 min on ice, washed, and then shifted to 37°C for the indicated chase times (hours), and lysed as detailed in MATERIALS AND METHODS. Biotinylated proteins were isolated using streptavidin beads, resolved in SDS-PAGE, and blotted with rabbit anti-Tac. Bar, 10 μm.

cells expressing Arf6-Q67L (Naslavsky *et al*., 2003). To provide additional evidence that CD59 and other GPI-APs followed the same trafficking pathway as MHCI and Tac, we examined whether the Arf6-Q67L block in trafficking had an impact on trafficking of Tac-GPI to late endosomes and lysosomes by monitoring degradation of an initial surface pool of biotinylated Tac-GPI. A substantial increase in the half-life of Tac-GPI was found in cells expressing Arf6-Q67L compared with cells expressing wild-type Arf6 (Figure 5E), similar to what was found for Tac and MHCI degradation (Naslavsky *et al*., 2003).

Arf6-Q67L Endosomes Accumulate Cholesterol and CD59, Blocking the Transfer to Rab5 Early Endosomes

Because internalization of CD59 and MHCI was sensitive to cholesterol sequestration by filipin treatment (Figures 2 and 4), we suspected that the endosomes that accumulate in cells expressing Arf6-Q67L would contain significant amounts of cholesterol. Indeed, these vacuolar structures contained internalized CD59 and labeled intensely with filipin (Figure 6A, compare filipin in transfected to untransfected cells). Filipin labeling in cells expressing Arf6-Q67L was on average nearly double that of untransfected cells (determined by measuring filipin fluorescence intensity per cell). These filipin-labeled structures represented PM cholesterol and not serum-derived cholesterol because filipin labeled these structures even in cells transfected with Arf6-Q67L in the absence of serum (our unpublished observations). Interestingly, the vacuoles, although heavily labeled with filipin, did not label with antibody to caveolin (Figure 6B) which remained evenly distributed primarily along the plasma membrane. Even overexpresssion of caveolin-GFP did not lead to labeling of Arf6-Q67L vacuoles with caveolin (our unpublished observations).

We showed previously that PM-associated Tac and Tac-GPI have distinct sensitivity to cold Triton X-100 extraction, with the latter being resistant (Naslavsky *et al*., 2003), and we showed here that total MHCI and CD59 behave like Tac and Tac-GPI, respectively (see Supplementary Figure 1). The presence of GPI-APs and cholesterol in the Arf6-Q67L endosomes raised the possibility that the GPI-APs would remain associated with cholesterol-rich rafts within these endosomes. We examined whether the GPI-APs sequestered in Arf6-Q67L endosomes would be resistant to Triton extraction. To help identify Arf6-Q67L–expressing cells, we coexpressed Tac-GPI. After 1-h internalization of Tac antibody, Tac-GPI was present in vacuoles that also labeled with Arf6 and filipin (Figure 7A). When these cells were treated with cold 1% Triton X-100 before fixation, Tac-GPI still remained in the enlarged structures that colabeled with filipin (Figure 7B), indicating that Tac-GPI and cholesterol pools within the Arf6-Q67L endosomes were detergent resistant. Arf6, by contrast, was completely extracted by the detergent (Figure 7B) as was MHCI (our unpublished observations).

The accumulation of CD59 in Arf6-Q67L-associated enlarged endosomes and protection from degradation of Tac-

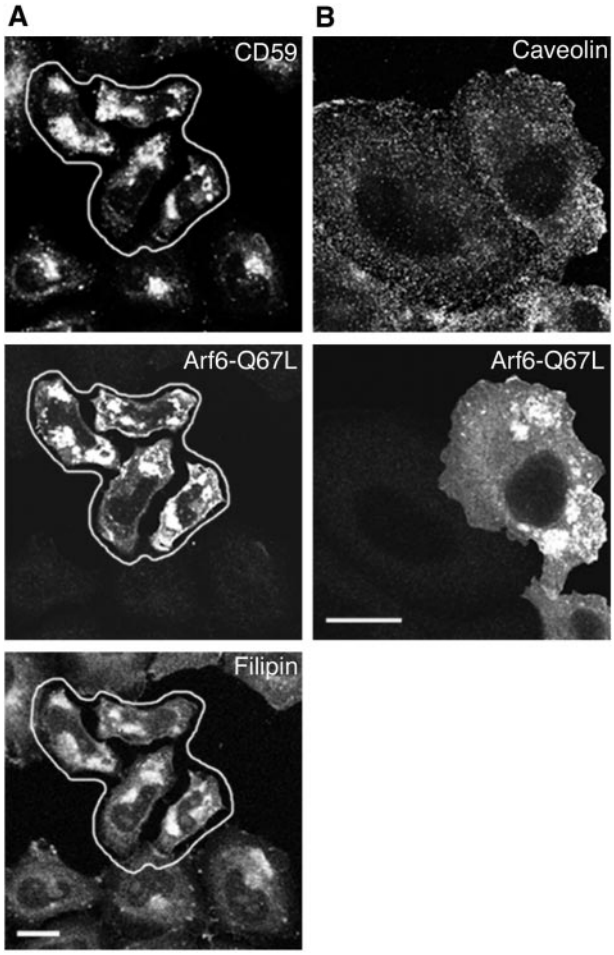

Figure 6. CD59 and cholesterol accumulate in Arf6-Q67L-associated vacuolar endosomes, devoid of caveolin-1. (A) Cells expressing Arf6-Q67L were incubated with anti-CD59 at 37°C for 1 h, and surface antibody was removed and then processed for immunofluorescence. After fixation, free cholesterol was stained with filipin as described in MATERIALS AND METHODS. Note the redistribution and intensity of filipin in the transfected cells (encircled). (B) Cells expressing Arf6-Q67L were labeled with antibody to caveolin-1. Bar, 10 μm.

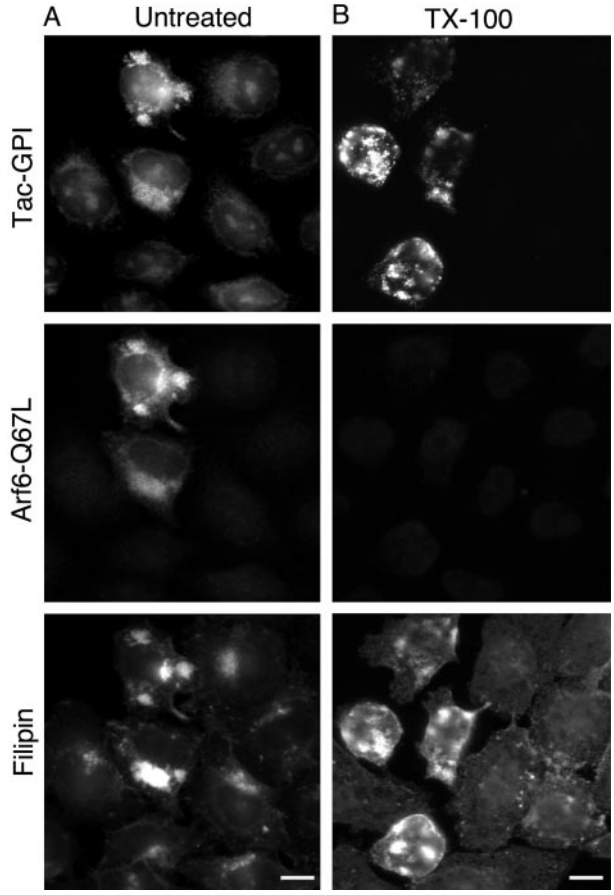

Figure 7. Tac-GPI, accumulated in Arf6-Q67L–induced vacuoles, is within detergent-resistant membranes. Cells coexpressing Arf6-Q67L and Tac-GPI were allowed to internalize anti-Tac antibody at 37°C for 1 h, cooled on ice, acid stripped, and incubated 3 min with ice-cold PBS (A) or with PBS and 1% TX-100 (B). After fixation, Arf6 was stained with polyclonal antibody. Tac-GPI was visualized with 488 Alexa goat anti-mouse, followed by staining of the free cholesterol with filipin. Bar, 10 μm.

GPI in cells expressing Arf6-Q67L (Figure 5) suggested that the transfer of CD59, like MHCI and Tac, to the Rab5-associated early endosome was inhibited in these cells. We previously showed that whereas Tac can accumulate in enlarged Rab5-associated structures in cells expressing the constitutively active Rab5 mutant (Q79L), in cells coexpressing Arf6-Q67 and Rab5-Q79L, Tac accumulates in the Arf6 early endosomal structures and does not converge with the Rab5-associated early endosomes (Naslavsky *et al*., 2003). Now, we investigated whether expression of Arf6-Q67L imposed a similar trafficking block for CD59. We found that whereas CD59 reached the enlarged Rab5 endosomes in cells expressing Rab5-Q79L alone (Figure 8A), CD59 was predominantly, although not exclusively, in Arf6-Q67L–associated endosomes in cells coexpressing both Rab5 and Arf6 active forms (Figure 8B), as was observed for MHCI (Naslavsky *et al*., 2003).

The block in delivery of cargo proteins to Rab5 early endosomes led us to ask whether endosomal cholesterol pools also would be altered in cells expressing Arf6-Q67L. Filipin colocalized with the enlarged Rab5-Q79L–associated endosomes in cells expressing Rab5-Q79L alone (Figure 8C). By contrast, filipin predominantly labeled Arf6-Q67L endosomes (Figure 8D, arrows) with very little associated with Rab5-Q79L endosomes (Figure 8D, arrowheads) in cells coexpressing both Arf6- and Rab5-activated forms.

DISCUSSION

GPI-APs and MHCI/Tac Share a Common Itinerary

In this study, we set out to determine whether detergent-resistant PM proteins follow a distinct pathway or a pathway shared by other PM proteins entering cells independently of clathrin. GPI-APs, both endogenous (CD59) and transfected (Tac-GPI), were chosen as representatives of a certain class of detergent-resistant PM proteins. Endogenous MHCI and expressed Tac represent transmembrane PM proteins that internalize independently of clathrin and travel through an endosomal system associated with Arf6. All of the GPI-APs examined entered in Arf6-associated endosomes and followed membrane trafficking pathways similar to MHCI and Tac. Furthermore, the internalization of both Tac-GPI and Tac required free cholesterol, occurred at the

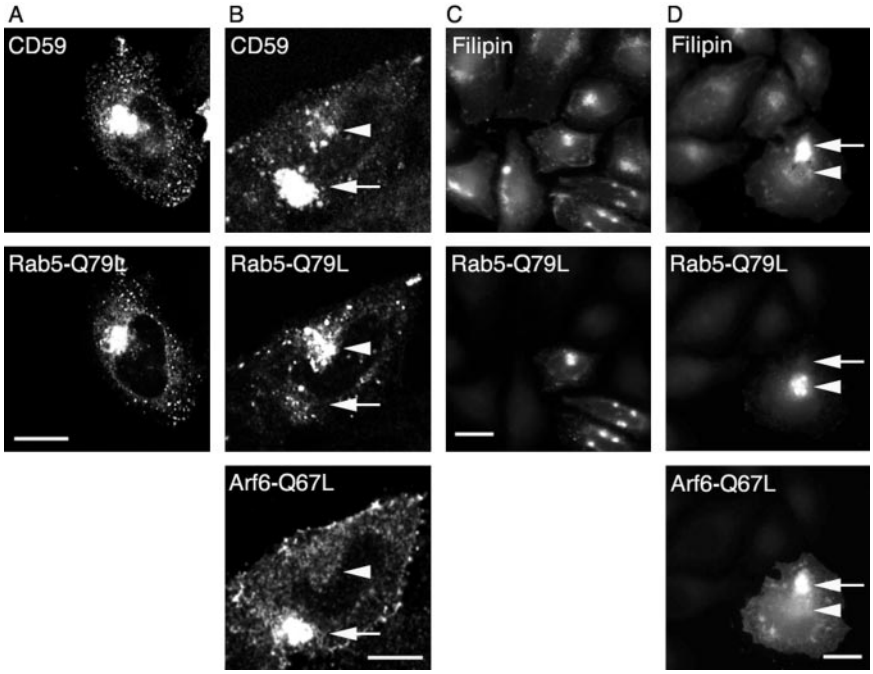

Figure 8. CD59 and cholesterol reach Rab5 compartment via Arf6-endosomes. HeLa cells were transfected with GFP-Rab5-Q79L alone (A and C) or with GFP-Rab5-Q79L and Arf6-Q67L (B and D). In A and B, cells were allowed to internalize phycoerythrin anti-CD59 antibody at 37°C for 1 h. In C and D, cells were fixed and stained with filipin. Bar, 10 μm.

same rate, and was stimulated to the same extent by activated Arf6. We suggest that GPI-AP are constitutively endocytosed along with other, clathrin-independent cargo proteins by similar endocytic mechanisms. Although no coat has as yet been identified with this endocytic event, the membrane lipid environment might be critical for this endocytic process.

In contrast to the GPI-APs, other proteins and toxins that associate with detergent-resistant membranes are internalized via caveolae. Caveolae have been found to mediate endocytosis for transcellular transport in endothelial cells (Oh *et al*., 1998), and during the uptake of autocrine motility factor (Benlimame *et al*., 1998), simian virus 40 (Pelkmans *et al*., 2001), and prion protein (Peters *et al*., 2003) into cells. We did not observe caveolin on vacuoles formed in cells expressing Arf6-Q67L (Figure 6) nor did we observe overexpressed caveolin-green fluorescent protein (GFP) labeling on any aspect of the Arf6 endosome (our unpublished observations). Toxins, such as cholera and shiga, bind raft-residing gangliosides and enter cells by a variety of endocytic mechanisms (Sandvig and van Deurs, 2002). Subsequent transport of these toxins to the endoplasmic reticulum via the Golgi requires that the toxins remain associated with detergent-resistant domains (Fujinaga *et al*., 2003). Intriguingly, although we could observe cholera toxin in enlarged Arf6-Q67L vacuoles, indicating that cholera toxin could enter cells with GPI-AP via this pathway, we never observed the toxin in the tubular, recycling membranes (our unpublished observations). Internalization of the heterotrimeric IL2 receptor, which contains Tac, the α chain, in addition to β and γ chains, seems to represent another variant requiring dynamin and Rho activity (Lamaze *et al*., 2001). How the β and γ chain alter the routing of Tac is not known.

The endosomal compartment that contains CD59 and GPI-APs, proteins that are resistant to detergent extraction, also contains integral membrane proteins such as MHCI that are readily solubilized. Intriguingly, both Triton-soluble and Triton-insoluble microdomains are present on the enlarged endosomes in cells expressing Arf6-Q67L. We know that these endosomes contain significant amounts of cholesterol (this study) and phosphatidylinositol bisphosphate (PIP_2) (Brown *et al*., 2001) and may be related to the common, early endosome-containing fluid and GPI-APs named GPI-AP early endosome compartment (Sabharanjak *et al*., 2002). Sabharanjak *et al.* (2002) found that GPI-AP endocytosis was dynamin independent and could be altered by expression of a dominant negative mutant of Cdc42. However, we did not observe any effect of expression of mutants of Cdc42, Rac, or Rho on the pattern of endocytosis of GPI-APs (our unpublished observations).

CD59 also was found in Arf6 tubular endosomal structures associated with the recycling of MHCI back to the PM (Radhakrishna and Donaldson, 1997; Caplan *et al*., 2002). These tubular endosomal structures labeled weakly with filipin (our unpublished observations) and contain PIP_2 (Brown *et al*., 2001). In HeLa cells, these recycling endosomes are devoid of transferrin receptor, although the tubular recycling membranes seem to emanate from a juxtanuclear structure that also contains transferrin receptor (our unpublished observations), suggesting that recycling may occur from a common sorting or recycling endosome. In Chinese hamster ovary (CHO) cells, GPI-AP recycles back to the PM along with the transferrin receptor (Mayor *et al*., 1998), suggesting that in CHO cells a shared recycling pathway is used. We do not know why a separate recycling pathway is found in some cell types (HeLa) and not in others (CHO), but this may reflect the diversity of membrane trafficking pathways observed in different cell types.

Cholesterol and PIP_2 Facilitate Clathrin-independent Endocytosis and Subsequent Trafficking

The Arf6-associated endosomes that carry both types of cargo contain cholesterol and PIP_2. These membrane lipids seem to be important for nonclathrin endocytic processes and may provide clues as to how clathrin-independent endocytosis occurs. The ability of filipin to inhibit selectively endocytosis of GPI-APs and MHCI/Tac, but not clathrin cargo, is significant and indicates that free cholesterol in the

membrane is required for endocytosis of these clathrin-independent cargo proteins. Cholesterol also has been shown to be required for membrane ruffling and subsequent macropinocytosis in A431 cells (Grimmer *et al*., 2002), processes likely to involve Arf6 activities (Brown *et al*., 2001; see below).

The stimulation of endocytosis of GPI-AP and MHCI/Tac in cells expressing Arf6-Q67L may be due to an elevation of PIP_2 at the PM. Arf6 functions in cells to regulate membrane traffic and cortical actin cytoskeleton through the stimulation of phosphatidylinositol 4-phosphate 5-kinase, the enzyme responsible for generating PM PIP_2 (Honda *et al*., 1999; Schafer *et al*., 2000; Brown *et al*., 2001). This kinase is present at the PM and on the Arf6 endosomal pathway and likely has basal activity in the absence of Arf6 stimulation (Brown *et al*., 2001); this may explain the lack of, or possibly mild inhibition of endocytosis in cells expressing Arf6-T27N. When Arf6 is constitutively active, however, increased local production of PIP_2 leads to a stimulation of the clathrin-independent endocytosis as we observed here. In Madin-Darby canine kidney cells, Arf6-Q67L expression led to enhanced internalization of both clathrin-dependent and independent mechanisms (Palacios *et al*., 2002), suggesting that the PIP_2 generated by active Arf6 can stimulate other endocytic pathways under certain conditions.

The juxtanuclear recycling compartment is thought to be an important pool of intracellular cholesterol (Hao *et al*., 2002). Our data suggest that Arf6-associated early endosomes provide a source of membrane cholesterol, connecting the PM pool with the recycling compartments. A significant amount of membrane cholesterol subsequently reaches Rab5/EEA1 early or sorting endosome as shown before (Holtta-Vuori *et al*., 2002). Some fraction of this membrane cholesterol is also returned to the PM via the tubular, Arf6 recycling system because we could detect some filipin labeling of the tubular endosomes (our unpublished observations). Although the enlarged endosomes obtained by activated Rab5 showed filipin labeling (Figure 8A), in cells coexpressing Arf6-Q67L the filipin labeled the Arf6- and not the Rab5-endosomes, demonstrating that a significant amount of PM cholesterol is sequentially delivered from Arf6 endosomes to Rab5 endosomes upon inactivation of Arf6. Expression of activated Rab11, a Rab associated with the juxtanuclear endocytic recycling compartment, also labels heavily with filipin (Hao *et al*., 2002; Holtta-Vuori *et al*., 2002), and it is likely that this compartment, like the Rab5 endosome, is also located downstream of the Arf6 early endosome. As noted by others (Gagescu *et al*., 2000; Fivaz *et al*., 2002; Maxfield, 2002; Sabharanjak *et al*., 2002; Edidin, 2003; Sharma *et al*., 2003) the variety of microdomains in these endosomal systems may provide a platform for differential sorting and trafficking of the cargo.

In summary, we found that PM proteins that are internalized independently of clathrin follow an endosomal system that is associated with Arf6. Both GPI-APs and integral membrane proteins such as MHCI and Tac enter together in cholesterol and PIP_2-containing membranes before their delivery to classical Rab5-associated endosomes. Their shared rates of endocytosis and itinerary indicate common mechanisms for endocytosis and provide a basis for understanding the mechanisms of endocytosis without clathrin.

ACKNOWLEDGMENTS

We thank J. Bonifacino, J. Lippincott-Schwartz, R. Lodge, M. McNiven, and W. Leonard for reagents, and S. Caplan, F. Brown, and E. Korn for critical comments on the manuscript.

REFERENCES

Awasthi-Kalia, M., Schnetkamp, P.P.M., and Deans, J.P. (2001). Differential effects of filipin and methyl-beta-cyclodextrin on B cell receptor signaling. Biochem. Biophys. Res. Commun. *287*, 77–82.

Benlimame, N., Le, P.U., and Nabi, I.R. (1998). Localization of autocrine motility factor receptor to caveolae and clathrin-independent internalization of its ligand to smooth endoplasmic reticulum. Mol. Biol. Cell *9*, 1773–1786.

Brown, D. (2002). Structure and function of membrane rafts. Int. J. Med. Microbiol. *291*, 433–437.

Brown, F.D., Rozelle, A.L., Yin, H.L., Balla, T., and Donaldson, J.G. (2001). Phosphatidylinositol 4,5-bisphosphate and Arf6-regulated membrane traffic. J. Cell Biol. *154*, 1007–1017.

Caplan, S., Naslavsky, N., Hartnell, L.M., Lodge, R., Polishchuk, R.S., Donaldson, J.G., and Bonifacino, J.S. (2002). A tubular EHD1-containing compartment involved in the recycling of major histocompatibility complex class I molecules to the plasma membrane. EMBO J. *21*, 2557–2567.

Conner, S.D., and Schmid, S.L. (2003). Regulated portals of entry into the cell. Nature *422*, 37–44.

Delahunty, M.D., Stafford, F.J., Yuan, L.C., Shaz, D., and Bonifacino, J.S. (1993). Uncleaved signals for glycosylphosphatidylinositol anchoring cause retention of precursor proteins in the endoplasmic-reticulum. J. Biol. Chem. *268*, 12017–12027.

Edidin, M. (2003). The state of lipid rafts: from model membranes to cells. Annu. Rev. Biophys. Biomol. Struct. *32*, 257–283.

Fivaz, M., Vilbois, F., Thurnheer, S., Pasquali, C., Abrami, L., Bickel, P.E., Parton, R.G., and van der Goot, F.G. (2002). Differential sorting and fate of endocytosed GPI-anchored proteins. EMBO J. *21*, 3989–4000.

Fujinaga, Y., Wolf, A.A., Rodighiero, C., Wheeler, H., Tsai, B., Allen, L., Jobling, M.G., Rapoport, T., Holmes, R.K., and Lencer, W.I. (2003). Gangliosides that associate with lipid rafts mediate transport of cholera and related toxins from the plasma membrane to endoplasmic reticulum. Mol. Biol. Cell *14*, 4783–4793.

Gagescu, R., Demaurex, N., Parton, R.G., Hunziker, W., Huber, L.A., and Gruenberg, J. (2000). The recycling endosome of Madin-Darby canine kidney cells is a mildly acidic compartment rich in raft components. Mol. Biol. Cell *11*, 2775–2791.

Grimmer, S., van Deurs, B., and Sandvig, K. (2002). Membrane ruffling and macropinocytosis in A431 cells require cholesterol. J. Cell Sci. *115*, 2953–2962.

Hao, M., Mukherjee, S., Sun, Y., and Maxfield, F.R. (2004). Effects of cholesterol depletion and increased lipid unsaturation on the properties of endocytic membranes. J. Biol. Chem. *279*, 14171–14178.

Hao, M.M., Lin, S.X., Karylowski, O.J., Wustner, D., McGraw, T.E., and Maxfield, F.R. (2002). Vesicular and non-vesicular sterol transport in living cells - The endocytic recycling compartment is a major sterol storage organelle. J. Biol. Chem. *277*, 609–617.

Holtta-Vuori, M., Tanhuanpaa, K., Mobius, W., Somerharju, P., and Ikonen, E. (2002). Modulation of cellular cholesterol transport and homeostasis by Rab11. Mol. Biol. Cell *13*, 3107–3122.

Honda, A., *et al*. (1999). Phosphatidylinositol 4-phosphate 5-kinase alpha is a downstream effector of the small G protein ARF6 in membrane ruffle formation. Cell *99*, 521–532.

Ikonen, E. (2001). Roles of lipid rafts in membrane transport. Curr. Opin. Cell Biol. *13*, 470–477.

Johannes, L., and Lamaze, C. (2002). Clathrin-dependent or not: is it still the question? Traffic *3*, 443–451.

Kwik, J., Boyle, S., Fooksman, D., Margolis, L., Sheetz, M.P., and Edidin, M. (2003). Membrane cholesterol, lateral mobility, and the phosphatidylinositol 4,5-bisphosphate-dependent organization of cell actin. Proc. Natl. Acad. Sci. USA *100*, 13964–13969.

Lamaze, C., Dujeancourt, A., Baba, T., Lo, C.G., Benmerah, A., and Dautry-Varsat, A. (2001). Interleukin 2 receptors and detergent-resistant membrane domains define a clathrin-independent endocytic pathway. Mol. Cell *7*, 661–671.

Maxfield, F.R. (2002). Plasma membrane microdomains. Curr. Opin. Cell Biol. *14*, 483–487.

Mayor, S., Sabharanjak, S., and Maxfield, F.R. (1998). Cholesterol-dependent retention of GPI-anchored proteins in endosomes. EMBO J. *17*, 4626–4638.

Nabi, I.R., and Le, P.U. (2003). Caveolae/raft-dependent endocytosis. J. Cell Biol. *161*, 673–677.

Naslavsky, N., Weigert, R., and Donaldson, J.G. (2003). Convergence of non-clathrin- and clathrin-derived endosomes involves Arf6 inactivation and changes in phosphoinositides. Mol. Biol. Cell *14*, 417–431.

Nichols, B.J., Kenworthy, A.K., Polishchuk, R.S., Lodge, R., Roberts, T.H., Hirschberg, K., Phair, R.D., and Lippincott-Schwartz, J. (2001). Rapid cycling of lipid raft markers between the cell surface and Golgi complex. J. Cell Biol. *153*, 529–541.

Oh, P., McIntosh, D.P., and Schnitzer, J.E. (1998). Dynamin at the neck of caveolae mediates their budding to form transport vesicles by GTP-driven fission from the plasma membrane of endothelium. J. Cell Biol. *141*, 101–114.

Palacios, F., Schweitzer, J.K., Boshans, R.L., and D'Souza-Schorey, C. (2002). ARF6-GTP recruits Nm23–H1 to facilitate dynamin-mediated endocytosis during adherens junctions disassembly. Nat. Cell Biol. *4*, 929–936.

Parton, R.G., and Richards, A.A. (2003). Lipid rafts and caveolae as portals for endocytosis: new insights and common mechanisms. Traffic *4*, 724–738.

Paterson, A.D., Parton, R.G., Ferguson, C., Stow, J.L., and Yap, A.S. (2003). Characterization of E-cadherin endocytosis in isolated MCF-7 and Chinese hamster ovary cells: the initial fate of unbound e-cadherin. J. Biol. Chem. *278*, 21050–21057.

Pelkmans, L., Kartenbeck, J., and Helenius, A. (2001). Caveolar endocytosis of simian virus 40 reveals a new two-step vesicular-transport pathway to the ER. Nat. Cell Biol. *3*, 473–483.

Peters, P.J., *et al*. (2003). Trafficking of prion proteins through a caveolae-mediated endosomal pathway. J. Cell Biol. *162*, 703–717.

Powelka, A.M., Sun, J., Li, J., Gao, M., Shaw, L.M., Sonnenberg, A., and Hsu, V.W. (2004). Stimulation-dependent recycling of integrin beta1 regulated by ARF6 and Rab11. Traffic *5*, 20–36.

Radhakrishna, H., and Donaldson, J.G. (1997). ADP-ribosylation factor 6 regulates a novel plasma membrane recycling pathway. J. Cell Biol. *139*, 49–61.

Ricci, V., Galmiche, A., Doye, A., Necchi, V., Solcia, E., and Boquet, P. (2000). High cell sensitivity to *Helicobacter pylori* VacA toxin depends on a GPI-anchored protein and is not blocked by inhibition of the clathrin-mediated pathway of endocytosis. Mol. Biol. Cell *11*, 3897–3909.

Rodal, S.K., Skretting, G., Garred, O., Vilhardt, F., van Deurs, B., and Sandvig, K. (1999). Extraction of cholesterol with methyl-beta-cyclodextrin perturbs formation of clathrin-coated endocytic vesicles. Mol. Biol. Cell *10*, 961–974.

Sabharanjak, S., Sharma, P., Parton, R.G., and Mayor, S. (2002). GPI-anchored proteins are delivered to recycling endosomes via a distinct cdc42-regulated, clathrin-independent pinocytic pathway. Dev. Cell *2*, 411–423.

Sandvig, K., and van Deurs, B. (2002). Membrane traffic exploited by protein toxins. Annu. Rev. Cell Dev. Biol. *18*, 1–24.

Schafer, D.A., D'Souza-Schorey, C., and Cooper, J.A. (2000). Actin assembly at membranes controlled by ARF6. Traffic *1*, 892–903.

Sharma, D.K., Choudhury, A., Singh, R.D., Wheatley, C.L., Marks, D.L., and Pagano, R.E. (2003). Glycosphingolipids internalized via caveolar-related endocytosis rapidly merge with the clathrin pathway in early endosomes and form microdomains for recycling. J. Biol. Chem. *278*, 7564–7572.

Skretting, G., Torgersen, M.L., van Deurs, B., and Sandvig, K. (1999). Endocytic mechanisms responsible for uptake of GPI-linked diphtheria toxin receptor. J. Cell Sci. *112*, 3899–3909.

Slepnev, V.I., and De Camilli, P. (2000). Accessory factors in clathrin-dependent synaptic vesicle endocytosis. Nat. Rev. Neurosci. *1*, 161–172.

Song, J., Khachikian, Z., Radhakrishna, H., and Donaldson, J.G. (1998). Localization of endogenous ARF6 to sites of cortical actin rearrangement and involvement of ARF6 in cell spreading. J. Cell Sci. *111*, 2257–2267.

Torgersen, M.L., Skretting, G., van Deurs, B., and Sandvig, K. (2001). Internalization of cholera toxin by different endocytic mechanisms. J. Cell Sci. *114*, 3737–3747.

Zhao, X.H., Greener, T., Al-Hasani, H., Cushman, S.W., Eisenberg, E., and Greene, L.E. (2001). Expression of auxilin or AP180 inhibits endocytosis by mislocalizing clathrin: evidence for formation of nascent pits containing AP1 or AP2 but not clathrin. J. Cell Sci. *114*, 353–365.